Earth and Planetary Science Letters 279 (2009) 20–33

Contents lists available at ScienceDirect

Earth and Planetary Science Letters

journal homepage: www.elsevier.com/locate/epsl

Constraints on the depths and temperatures of basaltic magma generation on Earth and other terrestrial planets using new thermobarometers for mafic magmas

Cin-Ty A. Lee [a,*], Peter Luffi [a], Terry Plank [b], Heather Dalton [a], William P. Leeman [c]

[a] Department of Earth Science, MS-126, Rice University, 6100 Main St., Houston, TX 77005, USA
[b] Lamont-Doherty Earth Observatory, P. O. Box 1000, 61 Route 9W, Palisades, NY 10964-1000, USA
[c] Division of Earth Sciences, National Science Foundation, 4201 Wilson Blvd, Arlington, VA 22230, USA

ARTICLE INFO

Article history:
Received 31 July 2008
Received in revised form 21 November 2008
Accepted 9 December 2008
Available online 30 January 2009

Editor: L. Stixrude

Keywords:
Thermobarometry
Potential temperature
Partial melting
Basalt
Thermal state
Planetary differentiation

ABSTRACT

Basaltic magmatism is a common feature of dynamically active terrestrial planets. The compositions of basalts reflect the temperatures and pressures of magma generation, providing windows into a planet's thermal state. Here, we present new thermobarometers based on magma Si and Mg contents to estimate the pressures and temperatures of basaltic magma generation on Earth and other terrestrial planets. Melting on Earth is intimately tied to plate tectonics and occurs mostly at plate boundaries: mid-ocean ridges and subduction zones. Beneath ridges, melting is driven by adiabatic decompression of passively upwelling mantle at 1300–1400 °C. Similar temperatures of melting are found for some arcs, suggesting that decompression melting is also important in arcs and that enhanced melting by hydrous fluxing is superimposed on this background. However, in arcs where melting temperatures are low (1200 °C), hydrous fluxing is required. Temperatures hotter than ridges (>1400 °C) are primarily found away from plate boundaries: beneath thick continental lithosphere and oceanic "hotspots" like Hawaii. Oceanic "hotspots" are thought to derive from deep thermal upwellings ("plumes"), but some hot anomalies beneath continents are not associated with deep-seated plumes and hence must have different origins, such as thermal insulation or radioactive heating of metasomatized zones. Melting on Venus, as constrained from spectral data of its surface, occurs at higher temperatures (1500 °C) and pressures than on Earth, perhaps because Venus is characterized by a thick and stagnant upper thermal boundary layer that retards convective heat loss. In this regard, Venus' upper thermal boundary layer may be analogous to thick continents on Earth. Mars appears to have cooled off to <1300 °C within its first billion years, but considerable controversy exists over the interpretation of young (<500 My) basaltic meteorites that record temperatures of 1550 °C. As for the first billion years of Earth's history, its upper mantle was hotter than 1700 °C, hence melting commenced at pressures greater than 7 GPa, where melts could have been denser than residual solids, resulting in downward fertilization of the Earth's mantle.

1. Introduction

Active basaltic volcanism is the surest indication that a planet is still dynamically active (BVSP, 1981). The melting that drives volcanism signifies that primordial or radioactively generated heat is being lost from the interior of the planet. Melting itself is one of the fundamental processes that drive planetary differentiation, that is, the gradual segregation of a planet into different compositional layers. For example, Earth's oceanic and continental crusts are ultimately the by-products of partial melting of the mantle. Because the compositions of melts are influenced by the thermal state of a planet, magmas can be used as records of the thermal and dynamic evolution of planetary interiors. In this paper, we use thermobarometric approaches to constrain the temperatures and pressures of melt extraction on Earth and different planetary bodies. Our results are used to discuss the origins of basaltic magmatism in the solar system.

2. Estimating pressure and temperature of mantle melting

Attempts to estimate the temperatures and pressures of melting have been relatively successful for the Earth's mid-ocean ridges (Klein and Langmuir, 1987; Langmuir et al., 1992; Plank and Langmuir, 1992). For example, the temperatures of mid-ocean ridge basalt (MORB) source regions in the mantle are determined by the distribution of Fe and Mg between olivine (a common liquidus phase of basaltic magmas) and basaltic melt (Roeder and Emslie, 1970; Beattie, 1993; Gudfinnsson and Presnall, 2001; Herzberg and O'Hara, 2002; Putirka, 2005; Herzberg et al., 2007; Putirka et al., 2007). In turn, the average pressure of melt extraction from the mantle is determined by estimating the average melting degree, which is itself determined by incompatible element ratio fractionations (Na/Ti, Sm/Yb) or relative

* Corresponding author. Tel.: +1 281 250 3606.
E-mail address: ctlee@rice.edu (C.-T.A. Lee).

0012-821X/$ – see front matter © 2008 Elsevier B.V. All rights reserved.
doi:10.1016/j.epsl.2008.12.020

enrichments in iron or highly incompatible (with respect to the solid residuum) minor or trace elements, such as Na and Ti, in the melt (Klein and Langmuir, 1987; Langmuir et al., 1992; Plank and Langmuir, 1992; Shen and Forsyth, 1995; Putirka, 1999). These thermobarometric approaches, however, are not as applicable to other planets or other tectonic regions because pressure estimates based on incompatible trace elements will be highly sensitive to the composition of the mantle source, which could vary considerably over different tectonic environments (as a result of metasomatic effects) or other planetary mantles. To broaden the range of applications, we refine and apply a SiO_2-based barometer, which is less sensitive to variations in mantle composition because silica, being a major element, is buffered at a given temperature and pressure by the mineralogy of the system. For example, the mantles of the terrestrial planets are largely ultramafic and hence dominated by olivine+orthopyroxene+clinopyroxene assemblages. In such assemblages, the SiO_2 activity of a melt is controlled by the presence of olivine and orthopyroxene via the reaction $Mg_2SiO_4^{ol}+SiO_2^{melt}=Mg_2Si_2O_6^{opx}$. The equilibrium constant for this reaction at a given temperature and pressure is given by

$$K(T,P)=\frac{a^{opx}_{Mg2Si2O6}}{a^{ol}_{Mg2SiO4}a^{melt}_{SiO2}} \quad (1)$$

where a represents the activity of the molecular component in a given phase. Because the Mg/(Mg+Fe) ratios of orthopyroxene and olivine are similar over the range of ultramafic compositions relevant to the generation of basaltic magmas, the ratio $\frac{a^{px}_{Mg2Si2O6}}{a^{ol}_{Mg2SiO4}}$ is relatively constant, which means that K scales inversely with silica ($K\sim\frac{1}{a^{melt}_{SiO2}}$) so that silica activity is buffered over a wide range of compositions at a given pressure and temperature (Carmichael et al., 1970). The molar volume change of this reaction is large (ΔV_{rxn}=−5.7 cm^3/mol at 1300 °C and 1 GPa), making silica activity pressure-sensitive (Carmichael et al., 1970; Albarède, 1992; Haase, 1996; Wang et al., 2002; Carmichael, 2004).

To calibrate the barometer, we assembled a database (with the aid of the LEPR database http://lepr.ofm-research.org) of 433 experimental basaltic liquid compositions in equilibrium with olivine and orthopyroxene ranging from pressures of 1 atm to 7 GPa and temperatures from 1100 to 1800 °C (see Appendix A for details). We note that olivine-orthopyroxene multiple saturation at high pressures (>4–5 GPa) near the fertile lherzolite solidus may only be valid over a limited range of melting conditions. Nevertheless, silica activity is still likely to be buffered because clinopyroxene is present on the solidus (our empirical calibrations should account for this). The compilation includes melts in peridotitic systems similar to those of model bulk silicate Earth compositions as well as Fe-rich and water-bearing systems, which are relevant to melting of Martian and Lunar mantles and hydrous melting in arcs on Earth. Fig. 1A shows the range of compositions (in wt.% and including H_2O) covered by our database. There is a general negative correlation between wt.% SiO_2 and pressure (Fig. 1B). Application of previous SiO_2-based barometers (Albarède, 1992; Haase, 1996) are also shown in Fig. 1C. These barometers do not successfully reproduce all the experimental data because they are parameterized primarily against wt.% SiO_2 rather than actual silica activity. As a consequence, instead of being largely independent of composition as noted above, these barometers are primarily applicable to the narrow compositional range they were calibrated against: low degree melts of mantle compositions similar to that of the bulk silicate Earth. These barometers were not intended for hydrous, unusually fertile or depleted mantle compositions that might characterize subduction-modified mantles on Earth or other planetary mantles. For example, water increases the SiO_2 wt.% (on an anhydrous basis) of the melt and significantly depresses the temperature of melting (Carmichael et al., 1970; Ulmer, 2001; Grove et al., 2002; Carmichael, 2004).

To broaden the applicability of the silica activity barometer, we first expressed magma compositions in terms of mol% of molecular species rather than in wt.% of metal oxides (mole fraction rather than wt.% better captures the effect of molecular species, such as H_2O, which have much lower molecular weights than the metal oxides). The silica activity is then approximated by accounting for the chemical interactions between different oxide components, that is, the silica activity is approximated by subtracting from the total silica the amount of silica that associates with other cations to form molecular species, such as ferromagnesian silicate and aluminosilicate species. Assuming oxide species on the 8 oxygen basis (Burnham, 1975; Ghiorso et al., 1983), we define the "silica index" as $Si_4O_8=0.25\times(SiO_2-0.5\times(FeO+MgO+CaO)-Na_2O-K_2O)$ (other oxide species are detailed in the Appendix A). The sensitivity of Si_4O_8 molecular species to pressure is better than that of wt.% SiO_2 (Fig. 1B). The following relationship was found to reproduce experimental P:

$$P=\frac{\ln(Si_4O_8)-4.019+0.0165(Fe_4Si_2O_8)+0.0005(Ca_4Si_2O_8)^2}{-770T^{-1}+0.0058T^{1/2}-0.003(H_{16}O_8)} \quad (2)$$

where Si_4O_8, $Fe_4Si_2O_8$, $Ca_4Si_2O_8$ and $H_{16}O_8$ are the mol% of those species in the liquid, P is in GPa, and $T(K)$ is temperature in Kelvin. The basic form of Eq. (2) was chosen to follow the thermodynamic expression of P as a function of Si_4O_8 and temperature, that is, $P=(a\ln Si_4O_8+b)T$, where a and b are constants that implicitly include the molar volume and entropy changes of the reaction; additional terms were incorporated into this functional form to yield Eq. (2). The $Fe_4Si_2O_8$ term accounts for anomalously Fe-rich basalts typical of Lunar or Martian magmas and the $Ca_4Si_2O_8$ term accounts for a slight compositional effect of Ca, and the extra temperature term ($T^{1/2}$) accounts for a slight non-linear dependence of Si_4O_8 on temperature. The effect of water is accounted for in the water term. Temperature is accounted for with the following thermometer:

$$T(^oC)=916.45+13.68(Mg_4Si_2O_8)+\frac{4580}{(Si_4O_8)}-0.509(H_{16}O_8)(Mg_4Si_2O_8) \quad (3)$$

where all molecular species are defined in the same way as in Eq. (2). Although there are already a number of robust thermometers based on Mg exchange between olivine and melt (Langmuir and Hanson, 1981; Ford et al., 1983; Beattie, 1993; Sugawara, 2000; Putirka, 2005; Putirka et al., 2007), this thermometer is internally consistent with our barometer and is simple to implement (see Appendix A for details).

The constant coefficients in Eq. (2) were not based on least squares regression of all the data to this formula because of non-uniform coverage of experimental data with pressure (large amounts of data in the 1–2 GPa pressure range, but few in the <1 and >3 GPa range). Instead, the constant coefficients were obtained by iteratively minimizing the misfits of Eq. (2) at different pressure intervals until there was no systematic correlation of misfit with pressure (experimental temperatures were assumed). An estimate of the uncertainties and systematic biases for Eq. (2) can be seen in Fig. 1C, where we plot the misfit, $P_{calc}-P_{exp}$. For 433 experiments, our barometer has an uncertainty of ±0.20 GPa, estimated by taking the average of the absolute residuals; such an uncertainty is best described as an approximation of 2 standard deviation uncertainty. Within this uncertainty, Eq. (2) has no systematic bias. Albarede's barometer has a total systematic bias of +0.031 GPa and an uncertainty of ±0.30 GPa, but pressures are overestimated slightly at <3 GPa and underestimated by up to 1 GPa at P>3 GPa; it also over-estimates pressure (by ~0.5 GPa) for Fe-rich compositions relevant to Martian and Lunar basalts. Haase et al.'s barometer has a systematic bias of +0.6 GPa and an uncertainty of ±1.0 GPa, but the bias can be >3 GPa for pressures <1

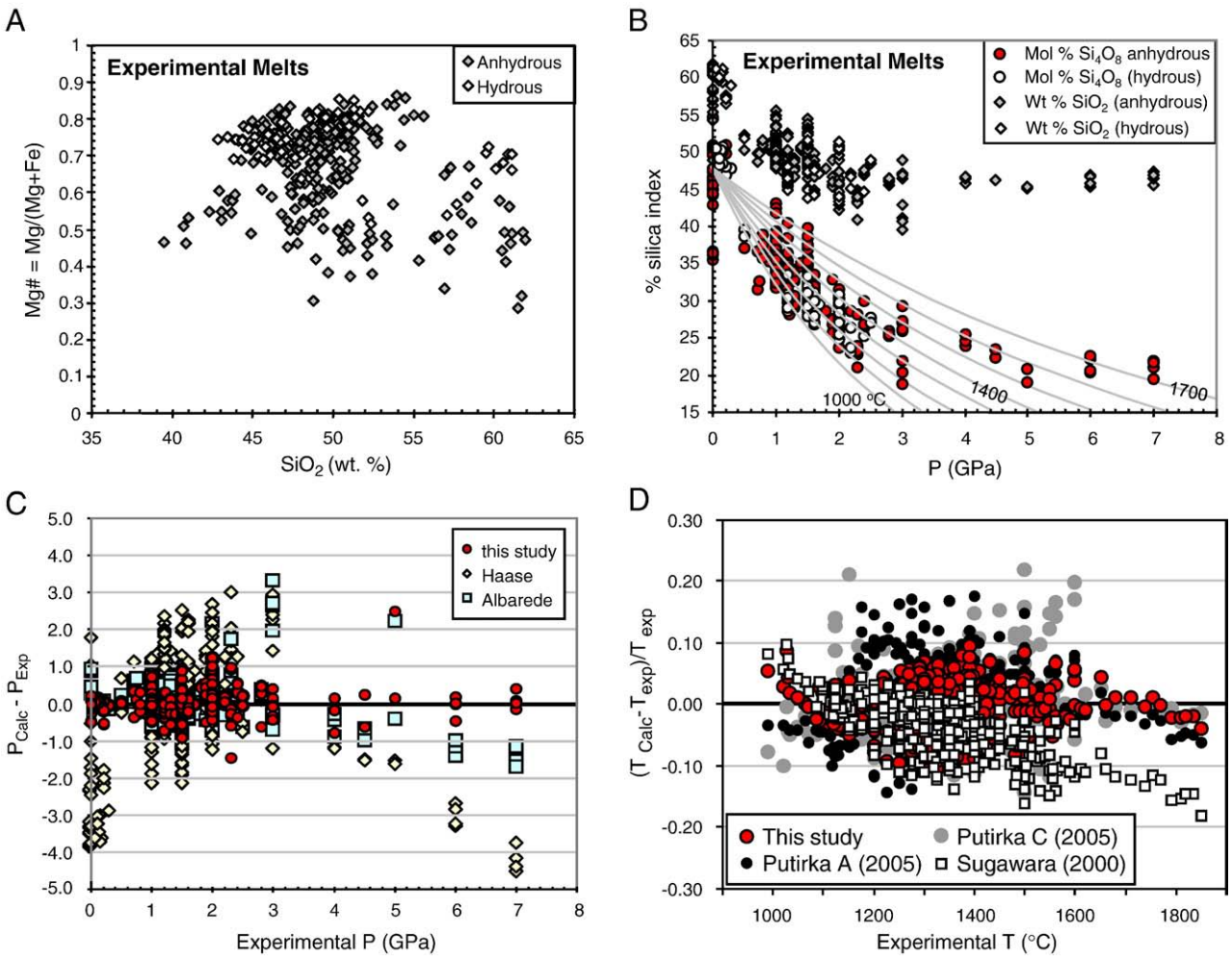

Fig. 1. Calibrations. A. This is the compositional range of experimental melts used in the barometer and thermometer calibrations (experimental data sources in Supplementary Online Materials). All melts are multiply saturated in olivine and orthopyroxene. Open symbols represent hydrous experiments and gray symbols represent anhydrous experiments. Mg# represents molar Mg/(Mg+Fe). B. Experimental melt compositions plotted against experimental pressure in GPa. Melt composition is expressed in terms of a silica index. Diamonds represent silica expressed in terms of SiO_2 wt.%. Circles represent silica expressed in terms of the Si_4O_8 molecular species minus the amount of Si tied up with Mg, Fe, and Ca in the melt. Open symbols represent hydrous experiments. Curved lines represent temperature contours estimated from Eq. (2). C. Calculated pressures minus experimental pressures plotted against experimental pressures. Red-filled circles represent this study. Other symbols represent previous barometers (Albarède, 1992; Haase, 1996; Wang et al., 2002). D. Calculated temperature minus experimental temperature using Eq. (4). Hydrous experiments are shown as open symbols. Insets represent similar plots, but temperatures are calculated using other thermometers (Sugawara, 2000; Putirka, 2005; Putirka et al., 2007).

and >3 GPa. The uncertainties in temperature are ±3% (corresponding to ~40 ° for a temperature of 1400 °C; Fig. 1D). This uncertainty is comparable to uncertainties reported for other thermometers. Our thermometer and barometer should be applicable to a broader range of basaltic compositions than most previous studies. However, these thermobarometers should not be applied outside of the range of experimental compositions used in our calibrations (see Fig. 1A and Appendix Fig. 1).

Successful application of Eqs. (2) and (3) in estimating conditions of melt generation/equilibration in the mantle requires knowledge of the primary magma composition, that is, the composition of the magma when it was last in equilibrium with the mantle. The other requisite is that both olivine and orthopyroxene be present in the mantle source as this assemblages buffers the silica activity in the magma (other phases can exist, but if olivine or pyroxene is not present, the barometer should not be applied because silica activity is not buffered according to Eq. (2)). Because all erupted magmas have gone through some degree of crustal-level crystal fractionation, the primary magma must be inferred by reversing the fractionation process. As in many previous studies (Leeman et al., 2005; Putirka, 2005; Herzberg et al., 2007), the approach taken here is to use magmas which have undergone olivine fractionation only. For terrestrial magmas, only magmas with MgO>8.5 wt.% were used. However, for komatiites and Hawaiian basalts, a minimum of 9 wt.% was used. Extraterrestrial basalts were treated differently as explained in their respective planetary sections.

Olivine increments in equilibrium with the instantaneous melt composition, assuming compositionally dependent olivine/melt $K_D(Fe/Mg)$ (Tamura et al., 2000), are then back-added to the magma until the magma composition reaches equilibrium with a mantle composition, assumed to be the average composition of the mantle residue after melt extraction (possible complications are discussed in the Appendix A). We provide in the Supplementary Online Materials a VisualBasic Excel Macro for fractionation correction and P-T calculation. The assumption is that the primary magma represents the aggregate of many melt increments generated along a polybaric melting path, and thus the P and T of this primary magma is taken to represent the weighted average P and T of the melting path (assuming no shallow-level re-equilibration) (Asimow and Longhi, 2004) or, alternatively, the P and T of shallow-level re-equilibration *in the mantle*. For all terrestrial magmas, we assumed a residual mantle composition equivalent to an olivine having an Mg#=Mg/(Mg+Fe)=0.9 (the Earth's mantle is thought to have an Mg#

of ~0.89; the value of 0.9 is taken as average that accounts for the effects of melt depletion). Extremely melt-depleted peridotites (Mg# up to 0.92) do exist in the mantle, but are most likely associated with the very last increment of melting along a decompressional melting path and therefore contribute very little to the aggregate melt that eventually erupts. In any case, if the average Mg# of the mantle residuum is higher than our assumed 0.9, our estimates of temperature and pressure are minimum estimates. If Mg#s of the residuum are 0.89 instead of 0.9, temperatures and pressures would be slightly lower. However, because the temperature sensitivity of the thermometer decreases with fertility (decrease in Mg#), the difference between temperatures using 0.89 and 0.9 is small (<20 °C). For all other planetary bodies except for Venus, measured magma compositions were taken as is (e.g., fractionation corrections were not done) because of uncertainties in the mantle composition and differentiation pathway. Except for Earth magmas, only the Venusian magma compositions were fractionation-corrected.

One important complication is the possibility of co-crystallization of two or more mineral phases (details in Appendix A). For example, small amounts of plagioclase or clinopyroxene could co-crystallize with olivine. Ignoring plagioclase results in a slight over-estimate of SiO_2 and MgO, giving slightly higher T and P. Ignoring clinopyroxene causes a slight under-estimate in SiO_2 and over-estimate of MgO, giving lower P and higher T. By considering only the most primitive magmas, however, these effects are minimized.

Finally, primary magma Ps and Ts are used to infer mantle potential temperatures, which is the temperature the mantle would have if it were adiabatically decompressed to the surface along a solid adiabat. This quantity forms a useful reference point to compare the temperatures of different regions of a planet. Potential temperatures are estimated by taking primary magma Ps and Ts and back-calculating along an isentropic melting path until the melting path intersects the solidus (the initial depth of melting) (McKenzie and Bickle, 1988; Katz et al., 2003). Extrapolation from this intersection point along a solid adiabat to the surface then yields the potential temperature of the mantle (red lines in Figs. 2–4 calculated after Katz et al., 2003).

3. Melting Earth's mantle

In this section, we apply these thermobarometers to different tectonic environments on Earth. Earth is unique among the planets in our solar system because it has an active interior and a mobile surface manifested in the form of plate tectonics. Below, we discuss how melting occurs in the various geologic environments found on our planet.

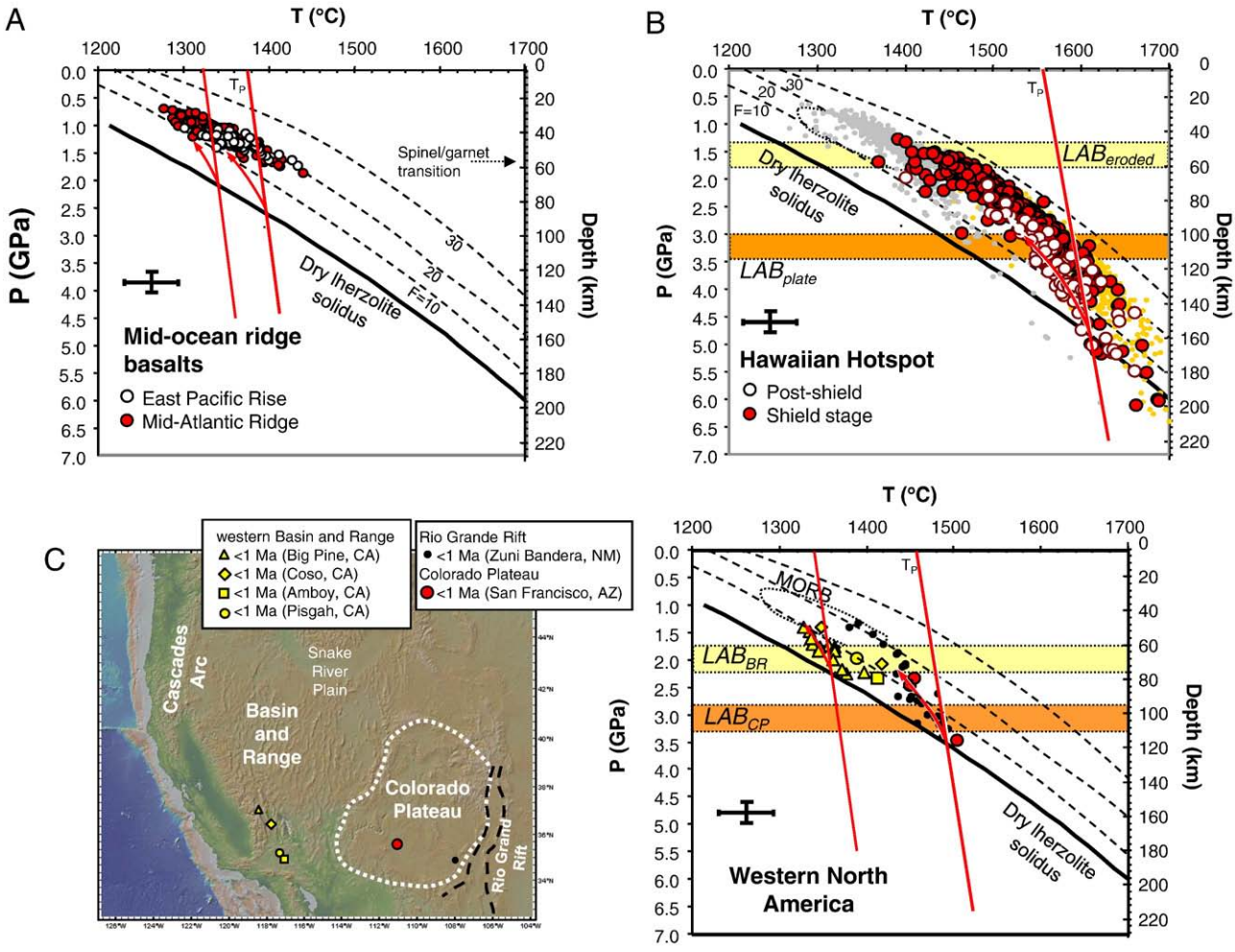

Fig. 2. A. Temperatures and pressures calculated for mid-ocean ridge basalts (MORBs) from the East Pacific Rise and mid-Atlantic Ridge (data from RidgePetDB). Lherzolite solidus and melt fraction isopleths are from Katz et al. (2003). Curved lines represent melting adiabats. Near-vertical lines (gray and red) represent solid mantle adiabats. B. Hawaiian hotspot source regions for shield and post-shield basalts (data are from the GEOROC database). C. Magma source regions in the western North America Cordillera: basalts are from the western Basin and Range (yellow), Rio Grande Rift (black dots) and Colorado Plateau (red symbols). Magmatic centers are shown on the map. Only basalts with MgO>9 wt.% were considered for A–C. All magma compositions in A–C were corrected for olivine-fractionation up to olivine Mg#s of 0.9 (Mg/(Mg+Fe)).

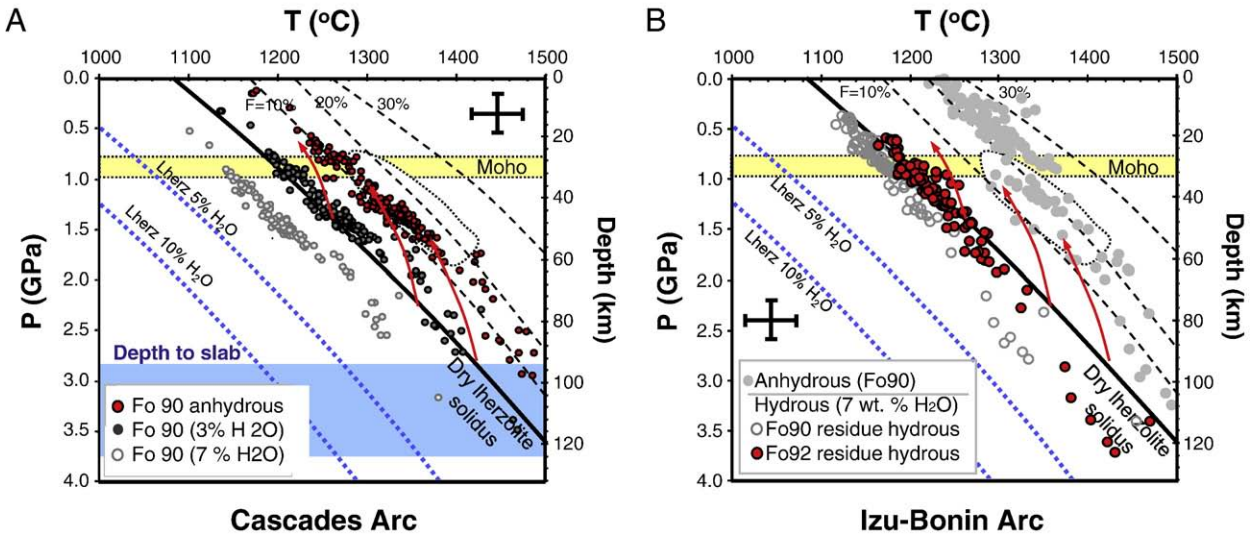

Fig. 3. Arc basalts (data from GEOROC). A. Temperatures and pressures of Cascades arc basalts (only basalts with MgO > 9 wt.% were used; olivine fractionation was corrected for until a target olivine Mg# of 0.90 was reached). Lherzolite solidi for varying water contents are taken from Katz et al. (2003). MORB field from Fig. 2A is shown. Horizontal gray line represents depth to the Juan de Fuca plate. B. Temperatures and pressures for boninites from the Izu-Bonin arc. Light gray symbols were estimated assuming perfectly anhydrous conditions and olivine-fractionation corrected up to olivine Mg# = 0.9. Dark gray circles represent calculations assuming 6 wt.% water in the melts and fractionation-corrected up to olivine Mg# = 0.90. Red circles represent calculations for 6 wt.% water in the melts and fractionat-correted up to olivine Mg# = 0.91. All data are compiled from the GEOROC database. Red lines with arrows correspond to isentropic melting adiabats.

3.1. Mid-ocean ridges

Mid-ocean ridges are plate boundaries, where most of the Earth's internal heat is liberated and crust forms (Fig. 2A). Melting beneath ridges is thought to be driven by adiabatic solid-state mantle upwelling (Klein and Langmuir, 1987; Shen and Forsyth, 1995) and, with the exception of ultra-slow spreading ridges, will be used here as a reference state to which all other tectonic environments will be compared. In fast spreading ridges, melting occurs over the pressure interval extending from the intersection of the adiabat with the mantle solidus to nearly the surface of the Earth (Klein and Langmuir, 1987; McKenzie and Bickle, 1988; Kinzler and Grove, 1992; Langmuir et al., 1992; Plank et al., 1995; Forsyth et al., 1998; Asimow et al., 2001; Asimow and Longhi, 2004). Taking mid-ocean ridge basalts (MORBs) from the mid-Atlantic ridge and East Pacific rise (>8.5 wt.% MgO) and assuming $Fe^{3+}/Fe = 0.1$ (Bezos and Humler, 2005) and final olivine Mg# = 0.9, we find that the temperatures and pressures of the primary magmas are respectively 1300–1400 °C and 0.7–1.7 GPa (30–50 km), falling systematically above the dry lherzolite solidus and the spinel-garnet transition (~50–60 km) as well as well below the base of the oceanic crust (~7 km) (Fig. 2A). Although the P-T data fall along an array, each data point should be considered independent of each other as they come from different ridge segments. Thus, rather than representing a melting array, we take each point to represent the temperature beneath a given ridge segment. Each of these points can be converted to a potential temperature by back-calculating along a melting adiabat until the solidus is reached (red lines in Fig. 2A are representative melting adiabats; (Katz et al., 2003)). The ridge data yield mantle potential temperatures around ~1350 °C (1300–1400 °C), which is significantly hotter than the 1280 °C once proposed (McKenzie, 1984; McKenzie and Bickle, 1988), but within error of recent estimates (Langmuir et al., 1992; Asimow et al., 2001; Courtier et al., 2007; Herzberg et al., 2007). Our temperatures are lower than those estimated by Putirka et al. (2007), who obtain 1400–1450 °C because we fractionation-correct the magmas to an olivine Mg# of 0.90 rather than 0.91 adopted by Putirka et al. (2007); an olivine Mg# of 0.91 is most likely an upper bound for the Mg# of the mantle residuum of MORBs.

Most of the pressures and temperatures plot on or slightly above the ~10% melt fraction contour of a dry fertile lherzolite, which is the temperature and pressure at which fertile lherzolite would melt by 10% (estimated from Katz et al., 2003); assuming a slightly depleted source like the mantle source of MORBs would yield a slightly higher solidus and lower melting degree (6–8%) in accordance with trace element constraints (Workman and Hart, 2005). The temperatures and pressures estimated here are comparable to those inferred from crustal thicknesses, incompatible element enrichments (e.g, Na),

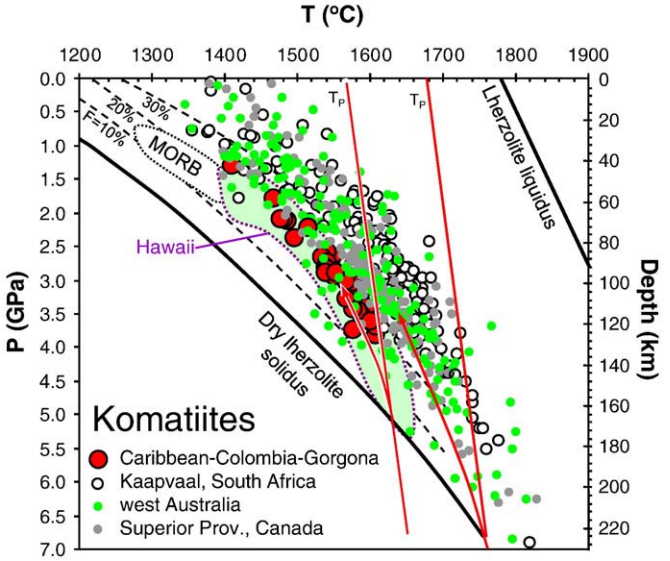

Fig. 4. Komatiites and basaltic komatiites from the Cretaceous Caribbean-Colombian oceanic plateau and Archean komatiite sections from the South Africa, west Australia, and the Superior craton in Canada (data from GEOROC). Other symbols as in Fig. 2. Fractionation correction up to olivine Mg# = 0.91 ($Fe^{3+}/Fe = 0.05$). Data compiled from GEOROC database. Red lines correspond to isentropic melting adiabat.

theoretical melting models, and geophysical constraints (Klein and Langmuir, 1987; Langmuir et al., 1992; Forsyth et al., 1998; Asimow et al., 2001). For the pressures we calculate, any higher temperatures (such as >1400 °C) would result in average melting fractions and crustal thicknesses inconsistent with observations, hence, our choice of olivine Mg#=0.90 and the resultant primary magma temperatures of ~1350 °C are reasonable. As for pressure, the 30–50 km depths of average equilibration inferred for primary MORBs are consistent with the notion that melt increments generated over a wide range in depth along the upwelling melting column are extracted fast enough to prevent complete re-equilibration of primary magmas at low pressures (<30 km). Application of our barometer to ultra-slow spreading ridges, where extension rates are comparable to conductive cooling rates, would be useful in assessing whether average melting pressures are influenced by spreading rate (Niu and O'Hara, 2008).

3.2. Subduction zones

At subduction zones, cold oceanic lithosphere sinks into the mantle and yet such regions (the arc) are characterized by large volcanic fluxes. The explanation for this is that melting in arcs is aided by dehydration of the subducting slab as it heats up, which releases fluids into the overlying mantle wedge and depresses the solidus (cf. Stolper and Newman, 1994; Kelley et al., 2006). To explore the thermal state of arcs, a global study of the temperatures and pressures of melting in arcs is needed. Here, we use two particular case studies to show how variable the thermal state of arcs can be.

We first examine the Cascades arc (Fig. 3A), where relatively young and presumably hot oceanic lithosphere of the Juan de Fuca plate subducts beneath North America. Olivine tholeiites, believed to derive from relatively dry mantle, were argued to form by shallow (70 km compared with >100 km to the surface of the subducting slab beneath the arc) and hot (1350–1450 °C) melting (Elkins Tanton et al., 2001; Leeman et al., 2005), which would be similar to melting conditions beneath mid-ocean ridges (see Fig. 2A). However, it has been suggested that the pre-eruptive water contents of Cascades basalts range from dry (<1 wt.% H_2O) to very wet (>8 wt.%) (Grove et al., 2002). In addition, it was pointed out that any prolonged presence of such high temperatures just beneath the arc crust (~35 km thick) would have caused extensive melting of the lower crust, but there is no evidence for such high degrees of melting so the high temperatures were thought to be transient (Elkins Tanton et al., 2001).

Our results are shown in Fig. 3A, where we consider magmas with >8.5 wt.% MgO and assume (Fe^{3+}/Fe=0.1 and final olivine Mg#=0.9). The effects of adding water on P and T are shown. Adding up to 7 wt.% H_2O increases calculated pressures by 0.4 GPa and decreases temperature by 150–200 °C (fractionation correction assumes mantle Mg# of 0.9) Regardless of water content, calculated pressures are mostly less than ~2 GPa, indicating that arc melting is shallow (<60 km) and occurs well above the subducting slab. Interpreting temperature calculations, however, is less straightforward. If pre-eruptive water contents are <1 wt.%, then melting occurred at hot temperatures (~1350 °C), similar to MORB-melting. If water contents were higher than 7 wt.%, cold (1150 °C) magmas are implied.

Unfortunately, the pre-eruptive water contents of arc basalts are often not known. Thus, if the pre-eruptive water contents indeed vary from <1 to >7 wt.% H_2O in the Cascades arc, strikingly different primary magma temperatures are implied and the temperature of the *melting* regime beneath the Cascades would hence vary by >200 °C. At a given location in the arc, this seems unlikely (although such temperature variations could occur in space and time). In addition, trace-element studies of Cascades arc lavas indicate that they are not highly enriched in fluid-mobile elements (Leeman et al., 2005), suggesting that their pre-eruptive water contents were probably not high. Moreover, in the next paragraph, we show that basalts formed in very hydrous environments have higher SiO_2 contents, which would give unreasonably low equilibration pressures (e.g., upper crustal depths) if they were erroneously considered dry. Whether we assume a wet or relatively dry environment for the Cascades arc magmas, our calculated equilibration pressures fall within the mantle and are hence reasonable. There is thus no strong evidence that the Cascades magmas on average were hydrous; Cascades arc magmas are hot. Like mid-ocean ridges, arc magmatism in the Cascades is probably driven mostly by hot and relatively dry decompression melting in the mantle wedge and is not limited by hydrous fluxing. The maximum temperatures are higher than geodynamic models of subduction using iso-viscous rheology in the mantle wedge (Peacock and Wang, 1999), but similar to the higher mantle wedge temperatures found in models using temperature-dependent rheologies (van Keken et al., 2002; Kelemen et al., 2003; Peacock et al., 2005). At least in the case of the Cascades, the effect of fluids is probably secondary in generating magmatism, but because of the high concentrations of fluid-mobile trace elements and water in the subducting slab, slab-derived fluids will influence the trace-element signature of arc magmas even if most of the melting occurred in a relatively dry environment.

In contrast to the hot Cascadian arc, magmas (basalts, basaltic-andesites, boninites) from the Izu-Bonin island arc in the western Pacific formed where old, cold Pacific lithosphere subducts beneath Eurasia (Arculus et al., 1992; Gill et al., 1992; Taylor et al., 1992). Again, because our knowledge of the pre-eruptive water contents of arc magmas is limited, we calculate Ps and Ts for a range of hypothetical water contents. In Fig. 3B, it can be seen that Ps and Ts calculated assuming anhydrous conditions (mantle Mg# of 0.9) yield many points that fall at pressures so low (0–1 GPa) that melting appears to occur in the crust and up to the surface of the Earth. This is clearly unreasonable. However, if the calculations are made with 7 wt.% water, deeper (but cooler) melting depths are obtained (Fig. 3B). Additional water would yield even more reasonable melting depths. Another way of achieving more reasonable melting depths (but less effective than adding water) is to assume a more refractory source; increasing from a lherzolitic residue of Mg# 0.9 to an extreme harzburgitic residue of Mg# 0.92 increases calculated pressures by 0.4 GPa (~15 km). Reasonable pressures are thus found only if Izu-Bonin arc magmas are assumed to be wet, which in turn indicates that melting temperatures of Izu-Bonin magmas were cold, possibly 200 °C cooler than melting beneath ridges and hot arcs like the Cascades. Our estimates of wet, shallow and cold melting for Izu-Bonin arc magmas lead us to conclude that melting here is not dominated by decompression of hot asthenosphere, but rather by hydrous flux melting of the base of the over-riding lithospheric mantle. The possibility that the melts derive from a more refractory source than MORB or other arcs is consistent with this interpretation.

In summary, the two examples discussed here illustrate how much the melting process beneath arcs can differ. Our case studies of the Cascades and Izu-Bonin arcs should by no means be taken as generalizations for hot and cold subduction zones. What is needed is a global study of arcs wherein the pressures and temperatures of melting and the relative contributions of hydrous flux melting to decompression melting are compared to the physical parameters of subduction zones, such as convergence rate and angle, slab age, and slab dip.

3.3. Intraplate magmatism

Magmatism on Earth also occurs away from plate boundaries. These include “hotspots”, a catch-all term describing relatively long-lived intraplate magmatic centers, and incipient rifts, a term used to describe continental interiors undergoing extension. There is ongoing debate on whether “hotspots” are indeed hot compared to mid-ocean ridges. Because many of these hotspots move significantly less than the plates themselves, the popular interpretation is that many “hotspots” are connected to deep thermal upwellings (e.g., plumes) anchored to the thermal boundary layer between the Earth's core and

mantle. The alternative explanation is that intraplate magmas derive from melting of more fertile and hence more easily fusible lithologies (e.g., pyroxenites) in a heterogeneous upper mantle and hence do not necessarily require deep thermal anomalies (Anderson, 2007). Fig. 2B shows P-T calculations for a well-known "hotspot", the Hawaiian volcanic chain in the Pacific (MgO>9 wt.%; $Fe^{3+}/Fe=0.1$, and final olivine Mg#=0.9). Although olivines with Mg#s>0.91 occur in the Hawaiian magmas, our choice of olivine Mg#=0.9 results in a minimum estimate of temperature, and therefore, a conservative estimate on the excess temperature the Hawaiian hotspot relative to MORB mantle.

Shield and post-shield phases are distinguished, the former representing the main volcanic edifice-building magmas and the latter representing the capping and post-erosional stage of magmatism, which is thought to represent the waning stages of magmatism after the Pacific plate moves off of the "hotspot" center and local mantle upwelling in response to flexural uplift caused by loading of Hawaiian volcanic chain on the Pacific lithosphere (Frey et al., 1990; Bianco et al., 2005). Again, taking the Mg# of the mantle residuum to be 0.9 (olivine phenocrysts in the Hawaiian picrites have Mg#s exceeding 0.9), we find that temperatures fall between 1450–1600 °C, forming an array beginning from 2.0 GPa (60 km) and intersecting the dry peridotite solidus at ~5 GPa or ~150–180 km. This intersection translates into a mantle potential temperature beneath Hawaii of ~1500–1600 °C, which is ~200 °C hotter than average MORB mantle or subarc mantle. Assuming a more forsteritic residuum (olivine Mg#=0.91) would increase excess temperatures by 50–100 °C (Putirka, 2005; Putirka et al., 2007).

Another key feature is that the highest pressure data points, corresponding to post-shield basalts, plot between the dry peridotite solidus and the base of the original Pacific lithosphere, indicating deep melting. In contrast, shield phase basalts appear to be shallower, falling within the original Pacific lithosphere itself, but coinciding with the depth of present lithosphere-asthenosphere boundary beneath Hawaii (Li et al., 2000). Collectively, this suggests that during the main shield building episodes, the lithospheric mantle was eroded and accompanied by high magmatic flux. The greater pressures of equilibration estimated for the post-shield phases might suggest relaxation of the deep lithosphere (re-thickening by conductive cooling), but over the short time interval between shield and post-shield phases (<5 My), extensive relaxation seems unlikely. A more likely possibility is that the mantle upwelling flux waned, suppressing the extent of decompression melting and thereby favoring the generation and extraction of deeper melts.

It is possible that our calculated temperatures are over-estimated if the source region of Hawaiian magmas is considerably more fertile than the ambient mantle as has been suggested by various investigators (Sobolev et al., 2005). However, assuming a slightly fertile mantle of Mg# 0.87 results in depths (Fig. 2B) that are much shallower than any geophysical estimates of the lithosphere-asthenosphere boundary (Li et al., 2000). In conclusion, the combination of high temperatures and evidence for eroded lithosphere strongly implies that the Hawaiian hotspot is driven by thermal anomalies. This alone, however, does not prove whether the thermal anomaly extends into the lower mantle (Courtier et al., 2007) and therefore does not prove the existence or absence of thermal plumes.

3.4. Continental magmatism

A second type of intraplate magmatism occurs beneath continents. One example is that of incipient continental extension in the North American Cordillera, where the Basin and Range province has been undergoing late Cenozoic extension, leading to decompression melting (Fig. 2C). In the western part of the Basin and Range, the region extending the fastest (Wernicke and Spencer, 1999), we find potential temperatures of 1350–1450 °C and pressures of melting between 2–3 GPa (60–90 km) (MgO>8.5 wt.%; $Fe^{3+}/Fe=0.1$, and final olivine Mg#=0.9). These temperatures are broadly consistent with those of Wang et al. (2002), who independently estimated temperatures and pressures in this region using Na and Fe contents (the Wang et al. temperatures and pressures in the central Basin and Range are much higher than those estimated here for the western Basin and Range, but our work-in-progress P-T estimates for central Basin and Range basalts are also high). Our pressure estimates also coincide with the shallow P-S conversions (60–80 km) seen in receiver function seismic studies for this region (Li et al., 2007) and are also consistent with surface wave studies in the region (Yang and Forsyth, 2006). These P-S conversions are thought by Li et al. to represent low velocity zones, and the coincidence with our melting depths suggests that these low velocity zones represent partial melt zones. The depths of melting further suggest that the lithosphere thickness in the western Basin and Range is relatively thin (~70 km), consistent with the notion that this region has undergone the most extension. By contrast, basaltic magmatism on the less extended Colorado Plateau and its margins (as represented by the San Francsico and Zuni-Bandera volcanic fields) yield higher pressures and temperatures (Fig. 2C). Surface wave tomography suggests that the lithosphere thickness beneath the Colorado Plateau is presently 120–150 km (West et al., 2004), which is similar to equilibration pressures of mantle xenoliths from the Colorado Plateau erupted in the Eocene (Smith, 2000; Lee et al., 2001). Thus, the deep lithosphere of the Colorado Plateau appears to have thinned considerably less than beneath the Basin and Range.

One intriguing observation is that the Colorado Plateau basalts intersect the solidus at temperatures consistent with a mantle potential temperature of ~1480 °C, which is hotter than that beneath mid-ocean ridges (Fig. 2A). Although these temperatures are not as hot as that recorded for Hawaii hotspot (Fig. 2B), they are similar to temperatures for other oceanic hotspots (Courtier et al., 2007). However, as far as we know, there is no evidence for a deep-seated thermal plume underneath this region, so these high temperatures are hard to explain. One possibility is that the insulating effects of thick continental lithosphere builds up heat beneath continents (Lenardic et al., 2005). A second possibility is that the high temperatures are caused by mantle return flow in response to Farallon plate subduction (Moucha et al., 2008). A third possibility is that the base of continental lithospheres becomes anomalously hot by radioactive heating associated with a highly metasomatized lower lithosphere.

3.5. Komatiites — window into the Archean

We end this section with a discussion of an uncommon class of rocks, known as komatiites. These are ultramafic magmas with MgO often greater than 20 wt.%. With the exception of the Cretaceous Gorgona komatiites associated with the Caribbean-Colombian oceanic plateau, nearly all komatiites are Archean (>2.5 Gy) in age. The high MgO contents of komatiites and associated basaltic komatiites in the Archean clearly indicate high temperatures. In Fig. 4, we have calculated Archean komatiite Ps and Ts assuming that the primary magma was dry and in equilibrium with a mantle having Mg# of 0.9. This gives Ps and Ts that fall on a hot melting adiabat, which crosses the solidus at ~7.0 GPa and 1750–1800 °C, corresponding to a solid mantle potential temperature of ~1700 °C. In all likelihood, the Mg# of the mantle residuum to komatiite generation was higher than 0.9, possibly as high as 0.93. If we correct back to 0.92, temperatures increase by 200 °C.

It has been argued that komatiites may be wet melts and that boninites might even be modern analogs of Archean komatiites (Parman et al., 1997; Grove and Parman, 2004), but this idea remains controversial (Arndt et al., 1998). However, a comparison of komatiite P-Ts (Fig. 4) with boninite P-Ts (Fig. 3B) shows that the water-free P-T estimates differ fundamentally. As discussed above, if boninites are assumed to be dry, ridiculously low pressures are obtained, but water-

free P-T estimates of komatiites give pressures well within the mantle, which are more reasonable. These differences stem from the fact that boninites have high Si contents whereas komatiites have much lower Si contents. In the case of boninites, the high Si contents are due to high water contents. The lack of high Si in komatiites suggests that they are nowhere near as wet as boninites. Recent investigations of the oxidation state of Fe in komatiite melt inclusions indicate that komatiites were likely dry (Berry et al., 2008). We thus take our dry-melting calculations as representative and conclude that komatiites formed by melting in a mantle with a potential temperature >1700 °C.

4. Melting on other terrestrial planetary bodies

To place Earth in context, we now explore basaltic magmatism on other planetary bodies. Meteorite and spectral data on other planetary bodies are limited, but the data are sufficient for developing first-order constraints on the thermal states of the Earth's Moon, Venus, Mars, and meteorite parent bodies.

4.1. The Earth's Moon

Beginning with small planetary bodies, such as the Earth's Moon, we calculated the P-Ts of Lunar basalts from Apollo 17 (Warner et al., 1975) and high Mg Lunar glasses (green picritic glasses) from Apollo 14B (Elkins et al., 2000) (Fig. 5A). No fractionation corrections were done (because the bulk composition of the lunar mantle is not known well), so the estimated P-Ts represent those of the measured magma compositions and would be analogous to multiple saturation experiments. If olivine fractionation has occurred, these P-Ts are minimum estimates (if significant plagioclase and pyroxene fractionation has occurred, they are maximum estimates). Apollo 17 basalts give temperatures between 1250-1380 °C and 0.7–2.0 GPa, the latter corresponding to a depth interval of 150–300 km on the Moon, and consistent with multiple saturation experiments of mare basalts (Longhi, 1992). Apollo 14 glasses yield much higher temperatures of 1550–1600 °C and pressures of 1.6–3.0 GPa (300–600 km), within error of multiple saturation experiments, which yield 1560 °C and 2.4 GPa (Elkins et al., 2000; Shearer et al., 2006). These depths of melting are much greater than on Earth. Given the small size of the Moon, these great depths require fundamentally different mechanisms for Lunar basalt generation. It has been suggested that Lunar basalt generation was due to degree-1 (hemispheric wavelength) convective overturn of a stratified Lunar mantle that had been emplaced by crystallization of the Lunar magma ocean (Hess and Parmentier, 1995; Zhong et al., 2000). The heat needed to generate the Lunar magma ocean is thought to be associated with the very origin of the Moon by the impacting of a giant body with the Earth within the first 30 My of Earth's history (Canup and Asphaug, 2001; Yin et al., 2002). Basaltic magmatism appears to have ended on the Moon by 3.8 Gy ago (Borg et al., 1999), marking the loss of most of its accretionary heat.

4.2. Vesta

Another small planetary body to consider is the eucrite parent body, which is thought to be the asteroid 4 Vesta (Fig. 5B). All basaltic eucrites (compiled from (Kitts and Lodders, 1998)) fall within error of 0 GPa (the artificially high pressures of two cumulate eucrites are

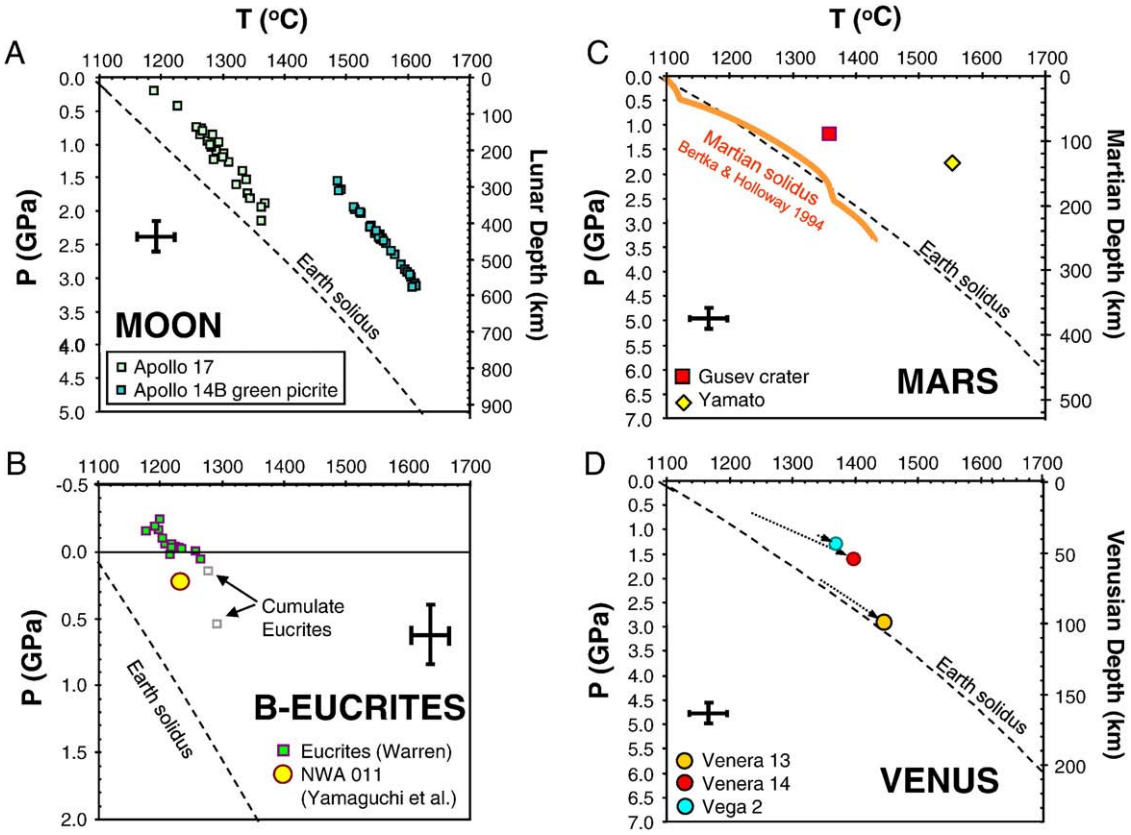

Fig. 5. Planetary magmas (data sources in text). A. Lunar basalt glasses (no fractionation correction). Apollo 14B glasses represent green picritic glasses. B. Eucrites (no fractionation correction). Eucrite with unusual oxygen isotopic composition (NWA 011) is shown with a yellow symbol (Yamaguchi et al., 2008). C. Martian basalts without fractionation correction. Meteorite Yamato 980459 is shown as a yellow diamond. Basaltic boulder from the Spirit Lander in Gusev crater is shown as red square. D. Venusian magmas based on Venera data (calculations were done with and without fractionation correction; the latter assumed final olivine Mg#=0.9). Fe^{3+}/Fe assumed to be 0 in all calculations.

shown to illustrate artifacts introduced by considering non-melt compositions) and 1180–1280 °C (no fractionation corrections were applied). These shallow pressures are consistent with eucrites deriving from a planet with very low gravitational acceleration, that is, a very small planetesimal, such as an asteroid. However, one meteorite previously classified on mineralogical and textural grounds as a eucrite (NWA 011; ref. (Yamaguchi et al., 2008)), yield higher pressures of 0.2 GPa. The oxygen isotopic composition of this meteorite differs from all other eucrites, leading Yamaguchi et al. (2008) to suggest it may have a different parent body than other eucrites. Our calculations also hint that the NWA 011 parent body may have been slightly larger than the eucrite parent body. In contrast to the Moon and the Earth, the small mass and gravity of planetesimals do not permit sufficient accretionary heat to be generated for differentiation yet many planetesimals are thought to have had magma oceans driven instead by heating from short-lived radionuclides, such as ^{26}Al, early in the Solar System's history (Bizzarro et al., 2005; Greenwood et al., 2005).

4.3. Mars

In comparison to planetesimals, larger planetary bodies, such as Mars, have enough accretionary and long-lived radioactive heat production to sustain a prolonged (Gy) dynamic interior. Of the many Martian meteorites known to exist, only two are thought to represent true liquids as all the rest are cumulates or peridotites. Of the two liquids, olivine phyric shergottite Yamato 980459 is the only one likely to represent a primitive melt (Musselwhite et al., 2006). Yamato 980459 is in equilibrium with olivine of Mg# 0.86 (Musselwhite et al., 2006), which is much higher than the inferred Mg# of the Martian mantle (0.75–0.8; (Bertka and Holloway, 1994)) and suggests that Yamato 980459 might represent a high degree (>50%) melt of the Martian mantle. We estimate equilibration T-Ps of 1550 °C and 1.7 GPa for Yamato 980459 (Fig. 5C; no fractionation correction applied), within error of multiple saturation experiments, which give T-Ps of 1540 °C and 1.2 GPa (Musselwhite et al., 2006). These P-Ts plot significantly above the inferred Martian solidus, confirming equilibrium with a very refractory source (Bertka and Holloway, 1994). An igneous crystallization age (Rb-Sr and Sm-Nd) of 472 Ma has been reported for this meteorite (Shih et al., 2005). If this age represents the age of magma extraction from the mantle, these temperatures are remarkably high considering that the Earth's mantle was already cooler by this time (1300–1400 °C).

To place the Yamato 980459 P-Ts in context, we turn to basaltic crusts from the Martian highlands, which are thought to be underlain by ancient (~4.5 Gy) crust as constrained by the high crater densities and radiometric ages of meteorites (cf. (Chen and Wasserburg, 1986; Borg et al., 1997; Blichert-Toft et al., 1999; Bouvier et al., 2005; Nimmo and Tanaka, 2005)). The Spirit Lander conducted spectral measurements of basaltic rocks in Gusev crater (McSween et al., 2006). These basalts are in equilibrium with olivine having Mg#s of 0.76–79, which is similar to that of the Martian mantle, and hence suggests that they could represent primary mantle-derived magmas. Our P-T estimates yield 1330 °C and 1.2 GPa (Fig. 5C; no fractionation correction), in agreement with the 1320 °C and 1.0 GPa determined from multiple saturation experiments (Monders et al., 2007). These temperatures are significantly lower than those inferred for Yamato 980459. If Gusev crater spectral data are representative, such data imply that the Martian mantle already cooled to Earth-like temperatures by ~4 Ga but the younger Yamato 980459 is hotter. This paradox can be reconciled if the high temperatures of Yamato 980459 record a later pulse of anomalously hot magmatism, but this would require the development of a mega-plume late in Mars history (Musselwhite et al., 2006). The high degrees of melting implied by the Yamato meteorite would suggest the production of large amounts of magmas, which would have resurfaced considerable portions of the planet. However, unlike Earth or Venus (see below), Mars' surface has not been significantly resurfaced. If, however, the young internal isochron ages of many Martian meteorites, such as Yamato 980459, are actually due to resetting by shock-induced melting or aqueous alteration (Bouvier et al., 2005), a late stage megaplume might not be required. If the Martian meteorites actually formed >4 Gy ago, as suggested by Bouvier et al. (Bouvier et al., 2005), much of the paradox would disappear. The true significance of Yamato 980459 will remain unknown until these different age interpretations are resolved.

4.4. Venus

Venus is the planet whose mass and density are most similar to Earth's (Fig. 5D). There are no meteorite samples from Venus, but the Russian Vega and Venera 13 and 14 missions acquired spectral data on the crust (Lodders and Fegley, 1998). Assuming that the major-element composition of the Venusian mantle is similar to that of Earth's (Lodders and Fegley, 1998), we corrected the Venusian spectral data for fractionation until a mantle source composition of Mg# of 0.9 was achieved. This yields temperatures of ~1350–1450 °C and pressures of 1.2 and 3.0 GPa, the latter corresponding to depths of 60 and 100 km (unfractionation-corrected P-Ts are also shown). Because the Venusian surface is considered to be young like Earth's surface (as inferred from the lack of crater preservation), these P-Ts might be representative of the recent thermal state of Venus. The Venusian P-Ts are slightly higher than mid-ocean ridge basalts on Earth, but are similar to basalts erupted through stagnant continental lithosphere on Earth, such as the basalts erupted through the Colorado Plateau discussed above (Fig. 2C). In this context, it is notable that convection in Venus is characterized by a stagnant lid (cf. (Nimmo and McKenzie, 1998)) and therefore its interior temperatures are predicted to be slightly higher than that of Earth's due to the insulating effects of a thick stagnant lid.

5. Epilogue

We end our tour of planetary magmatism with robust conclusions and open questions. Earth is a dynamic planet, resulting in a diversity of mantle melting environments and lithospheric thicknesses. The present average temperature of the Earth's mantle, as represented by passively upwelling mantle beneath mid-ocean ridges, is between 1300–1400 °C. At subduction zones where hot and young oceanic lithosphere descends back into the mantle, temperatures of the asthenospheric mantle wedge are nearly as hot as mid-ocean ridges, suggesting that arc magmatism, like mid-ocean ridge magmatism, is primarily driven by decompression associated with solid-state asthenospheric upwelling. The effect of water on depressing the solidus in arc environments appears to be superimposed on this background thermal field. However, in some arcs, magmas are clearly dominated by cold, water-fluxed melting, possibly involving the melting of the cold refractory lithospheric mantle of the overriding plate rather than the hot asthenospheric mantle wedge. Our observations provide tantalizing hints that the age, hence temperature, of the slab plays a role in dictating whether hydrous flux melting or decompression is the dominant driver of melting. However, the situation is likely to be much more complicated than anything we show here: slab dip, convergence rate, and slab age will all play a role. A global thermobarometric study of arc lavas, coupled with geochemistry and geophysical constraints, is clearly needed to resolve these questions and assess the generality of our case studies.

Temperatures higher than 1300–1400 °C on Earth are presently found beneath “hotspots”. These hot thermal anomalies are consistent with an origin by deep-seated thermal plumes. However, in order to truly test whether a correlation between hotspots and deep-seated thermal plumes exists, coupled petrologic studies of hotspot magmas with geophysical studies of the Earth's deep interior are needed. The only other tectonic environments on Earth where potential

temperatures presently exceed 1400 °C are under thick continental lithospheres and many of these have no obvious origin as thermal plumes. Is there another form of generating thermal anomalies that has been largely ignored? Could gradual heating beneath continents be due to the insulating effects of these conductive lids (Lenardic et al., 2005) or to radioactive heating associated with a metasomatized basal lithosphere enriched in heat-producing elements? To what extent could these processes also explain some hotspot magmatic centers in the middle of ocean basins?

Mars was certainly once active but appears to have started "dying" early on as our thermobarometry results suggest that the Martian mantle had already cooled to Earth-like temperatures (~1300 °C) within its first ~500 My. Convection may still be operating in Mars, but it is likely to be very sluggish, generating melts only occasionally. As for Venus, the modern mantle potential temperature is slightly hotter than Earth's, indicating that Venus is still quite active. This is not surprising as Venus is similar in size and density to the Earth, which because of its large size (compared to Mars) still contains enough primordial heat to drive convection. However, the slightly higher temperatures on Venus could imply a very different convective regime. Our barometric estimates suggest that the thickness of the Venusian lithosphere is ~100 km, within error of geophysical constraints (Nimmo and McKenzie, 1998). This, combined with the higher temperatures, is consistent with the hypothesis that convection on Venus is characterized by a stagnant "lid" or upper thermal boundary layer (Solomatov and Moresi, 1996). Earth, in contrast, is characterized by plate tectonics, and hence a mobile lid. Regardless of the origin of a stagnant lid (perhaps due to the absence of water (Campbell and Taylor, 1983; Nimmo and McKenzie, 1998)), it seems likely that Venus's non-convecting lid insulates its interior from heat loss, retarding the secular cooling of Venus compared to that of Earth. As for the Earth, lithospheres thicker than 100 km are found primarily beneath continents, which themselves are largely non-convecting and therefore could eventually heat up at depth as discussed above. It has been suggested that the long-term (Gy) stability and strength of some continental lithospheres on Earth is because they are made up of highly melt-depleted and dehydrated residual mantle material formed during an earlier melting event (Jordan, 1978; Pollack, 1986; Lee et al., 2005a,b). Melt depletion provides chemical buoyancy while dehydration increases the intrinsic viscosity of the mantle, two properties which collectively ensure that such lithospheres behave as rigid lids for the long term (Lenardic and Moresi, 1999). Could the Venusian lithosphere also be made up of dehydrated residual mantle? If so, did the Venusian lithosphere form by processes similar to the ones that created Earth's continental lithospheres?

Finally, Archean komatiites on Earth provide important constraints on Earth's early thermal state. Three billion years ago, the Earth's upper mantle appears to have been at least 1700 °C, e.g., 300–400 °C hotter than today. Such high temperatures also imply that melting initiates at great depths. At high pressures, melts become denser and may even become negatively buoyant with respect to the solid residuum (Stolper et al., 1981; Agee and Walker, 1993); this effect would only be amplified by the high Fe content of hot melts. In the modern Earth, melts are buoyant and rise up to form the crust and this is the dominant mechanism by which the silicate part of the Earth differentiates. However, in the early Archean, could the deeper melting fractions have segregated downward while the shallower melting fractions segregated upwards, the former causing upside-down differentiation and the latter generating the erupted komatiites that are now found in the crust? Could the dense, high pressure melt fractions have sunk, carrying highly incompatible elements, such as the heat-producing elements and the noble gases, into the transition zone and later remixed in solid-state form into the lower mantle? On small planetary bodies, this process would not occur due to the low gravity and hence low pressures. However, on planets larger than Earth, could such a process be the dominant mechanism of planetary differentiation?

Acknowledgments

We thank F. Albarede, J. Blichert-Toft, A. Lenardic, Q.-Z. Yin, B. Jacobsen, M. Manga, R. Dasgupta, P. Asimow, M. Collier, M. Blondes, J. H. Jones, Z.-X. A. Li, M. Hirschmann, S. Hart, and M. Jackson for discussions over the years it took us to start and finish this manuscript. We are grateful to P. Asimow and K. Putirka for their thoughtful and constructive reviews. This work was supported by NSF grants to Lee and Plank and a Packard Fellowship to Lee, but the views expressed here are independent of these funding agencies.

Appendix A. Calculating the silica index

Magma composition was re-expressed in terms of the following molecular species (on an 8 oxygen basis),

$$Si_4O_8 = 0.25 \times (SiO_2 - 0.5 \times (FeO + MgO + CaO) - Na_2O - K_2O)$$

$$Ti_4O_8 = 0.25 \times TiO_2$$

$$Al_{16/3}O_8 = 0.375 \times (Al_2O_3 - Na_2O)$$

$$Cr_{16/3}O_8 = 0.375 \times Cr_2O_3$$

$$Fe_{16/3}O_8 = 0.375 \times Fe_2O_3$$

$$Fe_4Si_2O_8 = 0.25 \times FeO$$

$$Mg_4Si_2O_8 = 0.25 \times MgO$$

$$Ca_4Si_2O_8 = 0.25 \times CaO$$

$$Na_2Al_2Si_2O_8 = Na_2O$$

$$K_2Al_2Si_2O_8 = K_2O$$

$$P_{16/5}O_8 = 0.625 \times P_2O_5$$

$$H_{16}O_8 = 0.125 \times H_2O$$

All oxide components are given in mol% (note Fe^{2+} and Fe^{3+} are treated separately), and all molecular species were re-normalized to 100%. To check for the robustness of Eq. (2), we plotted calculated pressures versus experimental pressures for different barometers (Fig. 1C). Correction factors in the form of additional compositional parameters were added on the basis of systematic biases with respect to composition. Appendix Fig. 1 shows that there are no systematic errors dependent on composition. In particular, there are no

systematic biases associated with alkali metals (Na and K). We note that our barometer over-estimates pressure for hydrous experiments involving melts with <2 wt.% H_2O, but reproduces hydrous experiments with >2 wt.% in the melt. This could be due to inadequate parameterization for the effects of water at low concentrations. However, it could also be due to the difficulty in measuring low water contents in experimental glasses.

Re-formulating olivine thermometry

The most recent thermometers are those of Putirka (2005) and Putirka et al. (2007), which are referred to here as the Putirka-2005 and Putirka-2007 thermometers, respectively. The Putirka-2005 thermometers have simple formulations and do a reasonable job reproducing the experimental temperatures in our database (see insets in Fig. 1D). The more recent Putirka-2007 thermometers were calibrated against a wider range of compositions and water content and shown by Putirka et al. (2007) to reproduce experimental data more successfully than the Putirka-2005 thermometers (as well as other published thermometers, such as those of Sugawara (2000)). The drawback of using the Putirka-2007 thermometers in conjunction with Eq. (2) is that there is a strong non-linear dependence on P, which when combined with the nonlinear dependence of P_L (Eq. (2)) and Si_4O_8 on T, makes the simultaneous solution of these two equations difficult and non-unique. Motivated by the need for a simpler thermometer, we developed a thermometer (Eq. (3)) that does not depend explicitly on P and that also uses the same speciation approach as in Eq. (2). Referring to Eq. (3) in the main text, the effect of pressure is captured indirectly by the third term involving the inverse of Si_4O_8 and the effect of water is accounted for by the fourth term. The reproducibility of T_L on experiments is as good as the Putirka-2005 thermometers, but has the advantages of being simple

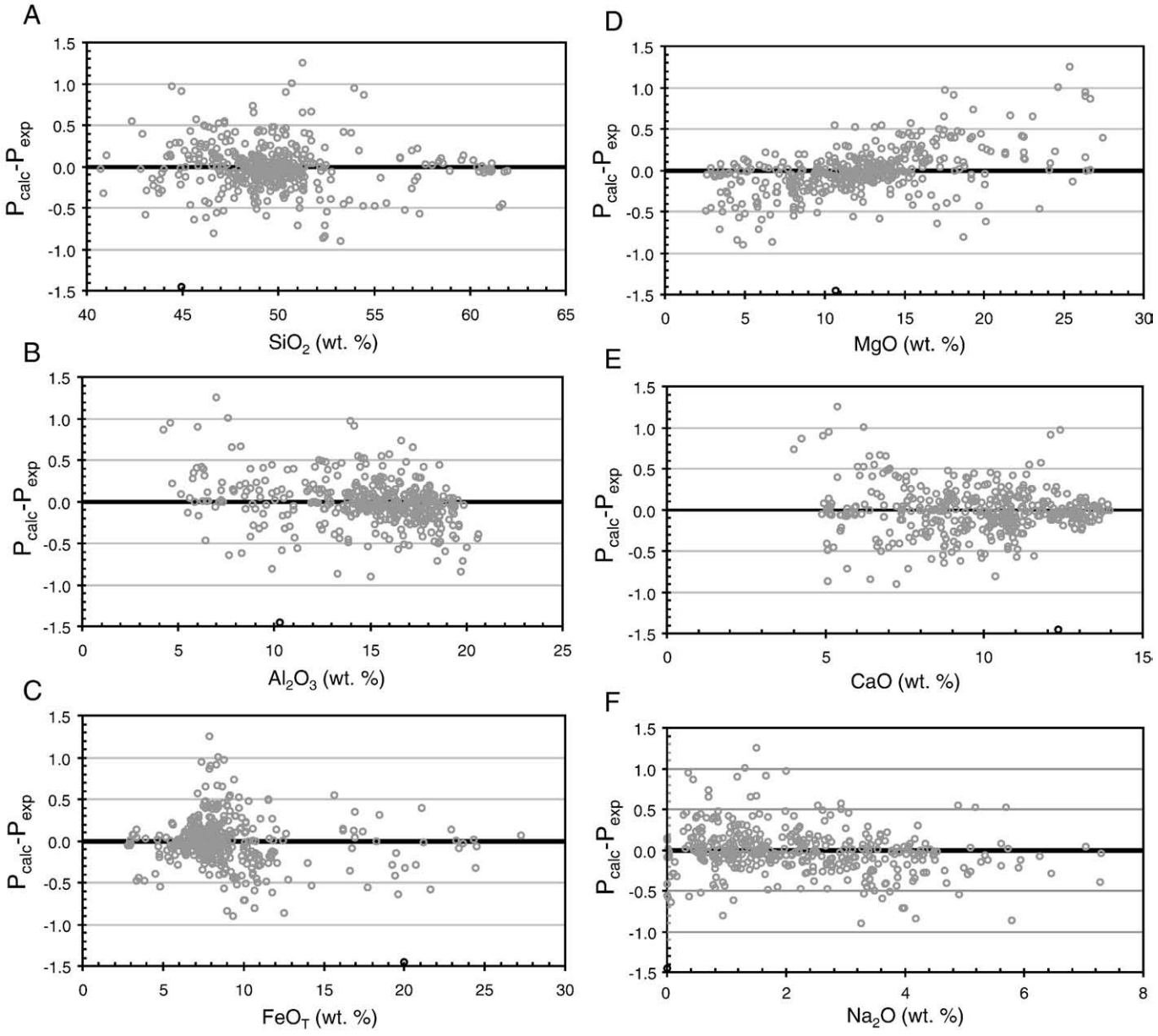

Appendix Fig. 1. Calculated pressures (assuming experimental T) minus experimental pressures versus various compositional indices. These figures show the range of composition over which the barometer and thermometer were calibrated.

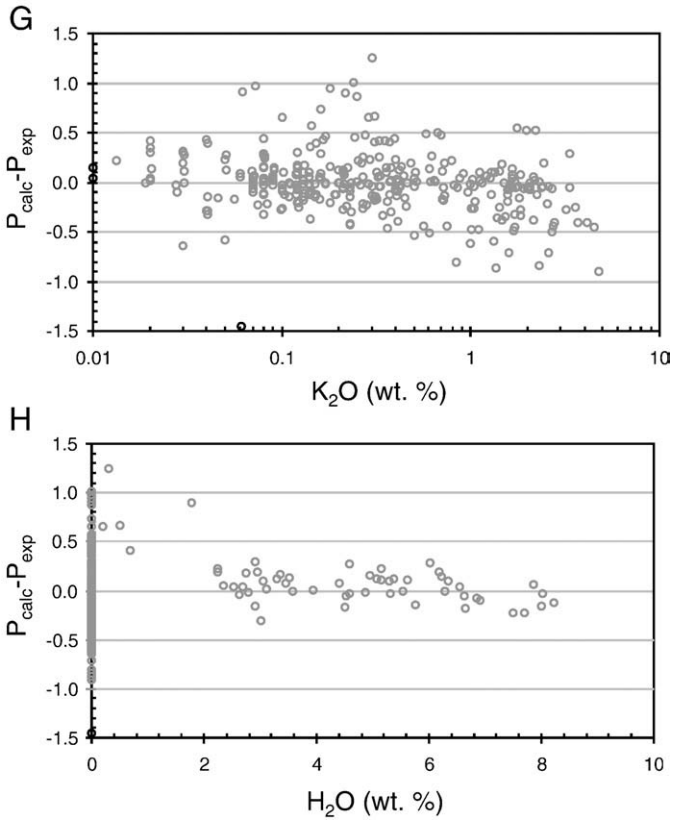

Appendix Fig. 1 (*continued*).

in formulation, internally consistent in choice of speciation, and not explicitly dependent on pressure (Fig. 1D).

Fractionation correction

Magmas are the integrated products of dynamic melting regimes and complicated melt transport processes (Langmuir et al., 1992; Asimow and Langmuir, 2003). Decompression melting initiated by solid-state upwelling results in melt increments being generated continuously along a path of changing pressure and temperature. Ideally, these melt increments pool together (for example, in magma chambers or mush zones) to generate an aggregate melt, whose composition represents a weighted average of the aggregated melt increments formed along the polybaric melting column (Langmuir et al., 1992; Plank et al., 1995; Asimow et al., 2001). This average composition reflects the weighted average P and T of melt generation. If on the other hand, the melts re-equilibrate at shallower depths, than the Ps and Ts represent shallow level re-equilibration temperatures.

Primary magma compositions must be calculated by correcting for low pressure fractionation. It is best to choose primitive (e.g., least fractionated; MgO>9.0 wt.%) magmas that have fractionated along olivine-control lines because more evolved magmas are multiply saturate, complicating fractionation correction. Olivine fractionation is corrected for by incrementally adding equilibrium olivine back into the magma until the magma is in equilibrium with olivine having a Mg# equivalent to the average mantle residuum using a composition-dependent $K_D^{ol/melt}=(Fe^{2+}/Mg)^{ol}/(Fe^{2+}/Mg)^{melt}$ (Tamura et al., 2000). A number of previous studies have followed the same approach (Leeman et al., 2005; Putirka, 2005; Courtier et al., 2007; Putirka et al., 2007).

An important variable in fractionation correction is the proportion of Fe^{3+} relative to Fe^{2+} in the magma. The Fe^{3+}/Fe_{total} ratio increases with oxygen fugacity fO_2 (Kress and Carmichael, 1991). For mid-ocean ridge and ocean island basalts, fO_2s are typically near the fayalite-magnetite-quartz (FMQ) buffer and hence have Fe^{3+}/Fe_{total} ~ 0.07–0.1. Arc magmas are generally thought to be more oxidized although by how much is still debated. The prevailing notion is that erupted arc magmas have fO_2s greater than 2–3 orders of magnitude higher than FMQ (Carmichael, 1991; Blatter and Carmichael, 1998), but recent studies of V/Sc systematics suggest that the mantle source regions of primitive arc magmas may only be slightly more oxidizing (up to 1–2 orders of magnitude greater than the FMQ buffer; (Lee et al., 2005a,b)) and that the oxidized nature of erupted magmas themselves may be due to self-oxidation imparted by water dissocation during magmatic differentiation or ascent (Holloway, 2004). Under-estimating fO_2 results in an over-estimate of temperature.

Conditions for applying the barometer and thermometer

A Visual Basic Excel Code for fractionation correction and P-T calculation is available on the Supplementary Online Materials as well as from the corresponding author upon request. Please follow these guidelines.

1. The barometer is only valid for primary mantle-derived magmas that were multiply saturated in olivine and orthopyroxene in their source regions. If the primary magma source does not have olivine and orthopyroxene, any P-T estimates by our approach will be meaningless. Although most planetary mantles are peridotitic and hence contain both of these phases, there is growing evidence that some terrestrial basaltic magmas might include a component derived from olivine-free sources, such as pyroxenites (Hirschmann et al., 2003; Sobolev et al., 2005; Herzberg, 2006). This degree of chemical heterogeneity falls outside the applicable compositional range of our thermobarometers.
2. One pitfall in our approach is the assumption of pure olivine fractionation. Some evolved magmas may be saturated in plagioclase or clinopyroxene in addition to olivine. Reversing crystal fractionation of such magmas is not trivial as the crystallizing proportions may not be known or may be difficult to estimate unless an entire differentiation suite is available. To avoid this problem, every attempt must be made to examine only those samples that are truly fractionated along olivine control lines. In addition, the most primitive magmas should be sought because the more primitive the magma is, the less the error introduced during fractionation correction.
3. The barometer has not been calibrated for silica-undersaturated rocks (<40 wt.% SiO_2) due to lack of sufficient experimental data, hence it is strongly advised not to apply our barometer to magmas, such as nephelinites, leucitites, kimberlites, etc. Our barometer also does not include the effects of CO_2 on silica activity. CO_2 is very important in the generation of silica-undersaturated melts and warrants future attention (Dasgupta and Hirschmann, 2006).

Appendix B. Supplementary data

Supplementary data associated with this article can be found, in the online version, at doi:10.1016/j.epsl.2008.12.020.

References

Agee, C.B., Walker, D., 1993. Olivine flotation in mantle melt. Earth Planet. Sci. Lett. 114, 315–324.
Albarède, F., 1992. How deep do common basaltic magmas form and differentiate? J. Geophys. Res. 97, 10997–11009.
Anderson, D.L., 2007. The eclogite engine: chemical geodynamics as a Galileo thermometer. In: Foulger, G.R., Jurdy, D.M. (Eds.), The Origins of Melting Anomalies: Plates, Plumes, and Planetary Processes.
Arculus, R.J., Pearce, J.A., Murton, B.J., van der Laan, S.R., 1992. Igneous stratigraphy and major-element geochemistry of Holes 786A and 786B. Proc. Ocean Drill. Program Sci. Results 125, 143–169.

Arndt, N., Ginibre, C., Chauvel, C., Albarede, F., Cheadle, M., Herzberg, C., Jenner, G., Lahaye, Y., 1998. Were komatiites wet? Geology 26, 739–742.
Asimow, P.D., Hirschmann, M.M., Stolper, E.M., 2001. Calculation of peridotite partial melting from thermodynamic models of minerals and melts, IV. Adiabatic decompression and the composition and mean properties of mid-ocean ridge basalts. J. Petrol. 42, 963–998.
Asimow, P.D., Langmuir, C.H., 2003. The importance of water to oceanic mantle melting regimes. Nature 421, 815–820.
Asimow, P.D., Longhi, J., 2004. The significance of multiple saturation points in the context of polybaric near-fractional melting. J. Petrol. 45, 2349–2367.
Beattie, P., 1993. Olivine-melt and orthopyroxene-melt equilibria. Contrib. Mineral. Petrol. 115, 103–111.
Berry, A.J., Danyushevsky, L.V., O'Neill, H.S.C., Newville, M., Sutton, S.R., 2008. Oxidation state of iron in komatiitic melt inclusions indicates hot Archaean mantle. Nature 455, 960–964.
Bertka, C.M., Holloway, J.R., 1994. Anhydrous partial melting of an iron-rich mantle I: subsolidus phase assemblages and partial melting phase relations at 10 to 30 kbar. Contrib. Mineral. Petrol. 115, 313–322.
Bezos, A., Humler, E., 2005. The Fe3+/Fe ratios of MORB glasses and their implications for mantle melting. Geochim. Cosmochim. Acta 69, 711–725.
Bianco, T.A., Ito, G., Becker, J.M., Garcia, M.O., 2005. Secondary Hawaiian volcanism formed by flexural arch decompression. Geochem. Geophys. Geosyst. 6. doi:10.1029/2005GC000945.
Bizzarro, M., Baker, J.A., Haack, H., Lundgaard, K.L., 2005. Rapid timescales for accretion and melting of differentiated planetesimals inferred from 26Al-26 Mg chronometry. Astrophys. J. Lett. 632, L41–L44.
Blatter, D.L., Carmichael, I.S.E., 1998. Hornblende peridotite xenoliths from central Mexico reveal the highly oxidized nature of subarc upper mantle. Geology 26, 1035–1038.
Blichert-Toft, J., Gleason, J.D., Telouk, P., Albarede, F., 1999. The Lu-Hf isotope geochemistry of shergottites and the evolution of the Martian mantle-crust system. Earth Planet. Sci. Lett. 173.
Borg, L., Norman, M., Nyquist, L.E., Bogard, D.D., Snyder, G., Taylor, L., Lindstrom, M.M., 1999. Isotopic studies of ferroan anorthosite 62236: a young lunar crustal rock from a light rare-earth-element-depleted source. Geochim. Cosmochim. Acta 63, 2679–2691.
Borg, L.E., Nyquist, L.E., Taylor, L.A., Wiesmann, H., Shih, C.-Y., 1997. Constraints on Martian differentiation processes from Rb-Sr and Sm-Nd isotopic analyses of teh basaltic shergottite QUE94201. Geochim. Cosmochim. Acta 61.
Bouvier, A., Blichert-Toft, J., Vervoort, J.D., Albarede, F., 2005. The age of SNC meteorites and the antiquity of the Martian surface. Earth Planet. Sci. Lett. 240, 221–233.
Burnham, C.W., 1975. Water and magmas; a mixing model. Geochim. Cosmochim. Acta 39, 1077–1084.
Basaltic Volcanism Study Project, 1981. Basaltic volcanism on the terrestrial planets. The Lunar and Planetary Institute. Pergammon Press, New York, 1286 p.
Campbell, I.H., Taylor, S.R., 1983. No water, no granites — no oceans, no continents. Geophys. Rese. Lett. 10, 1061–1064.
Canup, R.M., Asphaug, E., 2001. Origin of the Moon in a giant impact near the end of the Earth's formation. Nature 412, 708–712.
Carmichael, I.S.E., 1991. The redox states of basic and silicic magmas: a reflection of their source regions? Contrib. Mineral. Petrol. 106, 129–141.
Carmichael, I.S.E., 2004. The activity of silica, water, and the equilibration of intermediate and silicic magmas. Am. Mineral. 89, 1438–1446.
Carmichael, I.S.E., Nicholls, J., Smith, A.L., 1970. Silica activity in igneous rocks. Am. Mineral. 55, 246–263.
Chen, J.H., Wasserburg, G.J., 1986. Formation ages and evolution of Shergotty and its parent planet from U-Th-Pb systematics. Geochim. Cosmochim. Acta 50, 955–968.
Courtier, A.M., Jackson, M.G., Lawrence, J.F., Wang, Z., Lee, C.-T.A., Halama, R., Warren, J.M., Workman, R.K., Xu, W., Hirschmann, M.M., Larson, A.M., Hart, S.R., Lithgow-Bertelloni, C., Stixrude, L., Chen, W.-P., 2007. Correlation of seismic and petrologic thermometers suggests deep thermal anomalies beneath hotspots. Earth Planet. Sci. Lett. 264, 308–316.
Dasgupta, R., Hirschmann, M.M., 2006. Melting in the Earth's deep upper mantle caused by carbon dioxide. Nature 440, 659–662.
Elkins, L.T., Fernandes, V.A., Delano, J.W., Grove, T.L., 2000. Origin of lunar ultramafic green glasses: constraints from phase equilibrium studies. Geochim. Cosmochim. Acta 64, 2339–2350.
Elkins Tanton, L.T., Grove, T.L., Donnelly-Nolan, J.M., 2001. Hot, shallow mantle melting under the Cascades volcanic arc. Geology 29, 631–634.
Ford, C.E., Russell, D.G., Craven, J.A., Fisk, M.R., 1983. Olivine-liquid equilibria: temperature, pressure and composition dependence of the crystal/liquid cation partition coefficients for Mg, Fe2+, Ca and Mn. J. Petrol. 24, 256–265.
Forsyth, D.W., Scheirer, D.S., Webb, S.C., Dorman, L.M., Orcutt, J.A., Harding, A.J., Blackman, D.K., Morgan, J.P., Detrick, R.S., Shen, Y., Wolfe, C.J., Canales, J.P., Toomey, D.R., Sheehan, A.F., Solomon, S.C., Wilcock, W.S.D., 1998. Imaging the deep structure beneath a mid-ocean ridge: the MELT experiment. Science 280, 1215–1218.
Frey, F.A., Wise, W.S., Garcia, M.O., West, H., Kwon, S.-T., Kennedy, A.K., 1990. Evolution of Mauna Kea Volcano, Hawaii: petrologic and geochemical constraints on postshield volcanism. J. Geophys. Res. 95, 1271–1300.
Ghiorso, M.S., Carmichael, I.S.E., Rivers, M.L., Sack, R.O., 1983. The Gibbs free energy of mixing of natural silicate liquids; an expanded regular solution approximation for the calculation of magmatic intensive variables. Contrib. Mineral. Petrol. 84, 107–145.
Gill, J.B., Seales, C., Thompson, P., Hochstaedter, A.G., Dunlap, C., 1992. Petrology and geochemistry of Pliocene-Pleistocene volcanic rocks from the Izu arc, Leg 126. Proc. Ocean Drill. Program. Sci. Results 126, 383–404.
Greenwood, R.C., Franchi, I.A., Jambon, A., Buchanan, P.C., 2005. Widespread magma oceans on asteroidal bodies in the early Solar System. Nature 435, 916–918.
Grove, T.L., Parman, S.W., 2004. Thermal evolution of the Earth as recorded by komatiites. Earth Planet. Sci. Lett. 219, 173–187.
Grove, T.L., Parman, S.W., Bowring, S.A., Price, R.C., Baker, M.B., 2002. The role of an H_2O-rich fluid component in the generation of primitive basaltic andesites and andesites from the Mt. Shasta region, N California. Contrib. Mineral. Petrol. 142, 375–396.
Gudfinnsson, G.H., Presnall, D.C., 2001. A pressure-independent geothermometer for primitive mantle melts. J. Geophys. Res. 106, 16205–16211.
Haase, K., 1996. The relationship between the age of the lithosphere and the composition of oceanic magmas: constraints on partial melting, mantle sources and the thermal structure of the plates. Earth Planet. Sci. Lett. 144, 75–92.
Herzberg, C., 2006. Petrology and thermal structure of the Hawaiian plume from Mauna Kea volcano. Nature 444, 605–609.
Herzberg, C., O'Hara, M.J., 2002. Plume-associated ultramafic magmas of Phanerozoic age. J. Petrol. 43, 1857–1883.
Herzberg, C., Asimow, P.D., Arndt, N.T., Niu, Y., Lesher, C.M., Fitton, J.G., Cheadle, M.J., Saunders, A.D., 2007. Temperatures in ambient mantle and plumes: constraints from basalts, picrites and komatiites. Geochem. Geophys. Geosyst. 8. doi:10.1029/2006GC001390.
Hess, P.C., Parmentier, E.M., 1995. A model for the thermal and chemical evolution of the Moon's interior: implications for the onset of mare volcanism. Earth Planet. Sci. Lett. 134, 501–514.
Hirschmann, M.M., Kogiso, T., Baker, M.B., Stolper, E., 2003. Alkalic magmas generated by partial melting of garnet pyroxenite. Geology 31, 481–484.
Holloway, J.R., 2004. Redox reactions in seafloor basalts: possible insights into silicic hydrothermal systems. Chem. Geol. 210, 225–230.
Jordan, T.H., 1978. Composition and development of the continental tectosphere. Nature 274, 544–548.
Katz, R.F., Spiegelman, M., Langmuir, C.H., 2003. A new parameterization of hydrous mantle melting. Geochem. Geophys. Geosyst. 4. doi:10.1029/2002GC000433.
Kelemen, P.B., Rilling, J.L., Parmentier, E.M., Mehl, L., Hacker, B.R., 2003. Thermal structure due to solid-state flow in the mantle wedge beneath arcs. In: Eiler, J.M. (Ed.), Inside the subduction factory. Geophys. Monograph, vol. 138, pp. 293–311.
Kelley, K.A., Plank, T., Grove, T.L., Stolper, E.M., Newman, S., Hauri, E.H., 2006. Mantle melting as a function of water content beneath back-arc basins. J. Geophys. Res. 111. doi:10.1029/2005JB003732.
Kinzler, R.J., Grove, M., 1992. Primary magmas of mid-ocean ridge basalts 2. Applications. J. Geophys. Res. 97, 6907–6926.
Kitts, K., Lodders, K., 1998. Survey and evaluation of eucrite bulk compositions. Meteorit. Planet. Sci. 33, A197–A213.
Klein, E.M., Langmuir, C.H., 1987. Global correlations of ocean ridge basalt chemistry with axial depth and crustal thickness. J. Geophys. Res. 92, 8089–8115.
Kress, V.C., Carmichael, I.S.E., 1991. The compressibility of silicate liquids containing Fe_2O_3 and the effect of composition, temperature, oxygen fugacity and pressure on their redox states. Contrib. Mineral. Petrol. 108, 82–92.
Langmuir, C.H., Hanson, G.N., 1981. Calculating mineral-melt equilibria with stoichiometry, mass balance, and single component distribution coefficients. In: Newton, R.C., Navrotsky, A., Wood, B.J. (Eds.), Thermodynamics of Minerals and Melts. Springer, New York, pp. 247–271.
Langmuir, C., Klein, E.M., Plank, T. (Eds.), 1992. Petrological systematics of mid-ocean ridge basalts: constraints on melt generation beneath ocean ridges. American Geophysical Union. 183–280 pp.
Lee, C.-T.A., Leeman, W.P., Canil, D., Li, Z.-X.A., 2005a. Similar V/Sc systematics in MORB and arc basalts: implications for the oxygen fugacities of their mantle source regions. J. Petrol. 46, 2313–2336.
Lee, C.-T.A., Lenardic, A., Cooper, C.M., Niu, F., Levander, A., 2005b. The role of chemical boundary layers in regulating the thickness of continental and oceanic thermal boundary layers. Earth Planet. Sci. Lett. 230, 379–395.
Lee, C.-T., Yin, Q., Rudnick, R.L., Jacobsen, S.B., 2001. Preservation of ancient and fertile lithospheric mantle beneath the southwestern United States. Nature 411, 69–73.
Leeman, W.P., Lewis, J.F., Evarts, R.C., Conrey, R.M., Streck, M.J., 2005. Petrologic constraints on the thermal structure of the southern Washington Cascades. J. Volcanol. Geotherm. Res. 140, 67–105.
Lenardic, A., Moresi, L.N., 1999. Some thoughts on the stability of cratonic lithosphere; effects of buoyancy and viscosity. J. Geophys. Res., B, Solid Earth Planets 104, 12,747–712,759.
Lenardic, A., Moresi, L.-N., Jellinek, A.M., Manga, M., 2005. Continental insulation, mantle cooling, and the surface area of oceans and continents. Earth Planet. Sci. Lett. 234, 317–333.
Li, X., Kind, R., Priestley, K., Sobolev, S.V., Tilmann, F., Yuan, X., Weber, M., 2000. Mapping the Hawaiian plume with converted seismic waves. Nature 405, 938–941.
Li, X., Yuan, X., Kind, R., 2007. The lithosphere-asthenosphere boundary beneath the western United States. Geophys. J. Int. 170, 700–710.
Lodders, K., Fegley, J.B., 1998. The Planetary Scientist's Companion. Oxford University Press, Oxford. 371 pp.
Longhi, J., 1992. Experimental petrology and petrogenesis of mare volcanics. Geochim. Cosmochim. Acta 56, 2235–2251.
McKenzie, D., 1984. The generation and compaction of partially molten rock. J. Petrol. 25, 713–765.
McKenzie, D., Bickle, M.J., 1988. The volume and composition of melt generated by extension of the lithosphere. J. Petrol. 29, 625–679.
McSween Jr., H.Y., Wyatt, M.B., Gellert, R., Bell, J.F., Morris, R.V., Herkenhoff, K.E., Crumpler, L.S., Milam, K.A., Stockstill, K.R., Tornabene, L.L., Arvidson, R.E., Bartlett, P., Blaney, D., Cabrol, N.A., Christensen, P.R., Clark, B.C., Crisp, J.A., des Marais, D.J., Economou, T., Farmer, J.D., Farrand, W., Ghosh, A., Golombek, M., Greeley, R., Hamilton, V.E., Johnson, J.R., Joliff, B.L., Klingelhofer, G., Knudson, A.T., McLennan, S.M., Ming, D., Moersch, J.E.,

Rieder, R., Ruff, S.W., Schroder, C., deSouza, P.A., Squyres, S.W., Wanke, H., Wang, A., Yen, A., Zipfel, J., 2006. Characterization and petrologic interpretation of olivine-rich basalts at Gusev crater, Mars. J. Geophys. Res. 111. doi:10.1029/2005JE002477.
Monders, A.G., Medard, E., Grove, T.L., 2007. Phase equilibrium investigations of the Adirondack class basalts from the Gusev plains, Gusev crater, Mars. Meteorit. Planet. Sci. 42, 131–148.
Moucha, R., Forte, A.M., Rowley, D.B., Mitrovica, J.X., Simmons, N.A., Grand, S.P., 2008. Mantle convection and the recent evolution of the Colorado Plateau and the Rio Grande Rift valley. Geology 36, 439–442.
Musselwhite, D.S., Dalton, H.A., Kiefer, W.S., Treiman, A.H., 2006. Experimental petrology of the basaltic shergottite Yamato-980459: implications for the thermal structure of the Martian mantle. Meteorit. Planet. Sci. 41, 1271–1290.
Nimmo, F., McKenzie, D., 1998. Volcanism and tectonics on Venus. Annu. Rev. Earth Planet. Sci. 26, 23–51.
Nimmo, F., Tanaka, H., 2005. Early crustal evolution of Mars. Annu. Rev. Earth Planet. Sci. 33, 133–161.
Niu, Y., O'Hara, M.J., 2008. Global correlations of ocean ridge basalt chemistry with axial depth: a new perspective. J. Petrol. 49, 633–664.
Parman, S.W., Dann, J.C., Grove, T.L., de Wit, M.J., 1997. Emplacement conditions of komatiite magmas from the 3.49 Ga Komati formation, Barberton Greenstone Belt, South Africa. Earth Planet. Sci. Lett. 150, 303–323.
Peacock, S.M., Wang, K., 1999. Seismic consequences of warm versus cool subduction metamorphism: examples from southwest and northeast Japan. Science 286, 937–939.
Peacock, S.M., van Keken, P., Holloway, D., Hacker, B.R., Abers, G.A., Fergason, R.L., 2005. Thermal structure of Costa Ricea — Nicaragua subduction zone. Phys. Earth Planet. Int. 149, 187–200.
Plank, T., Langmuir, C., 1992. Effects of the melting regime on the composition of the oceanic crust. J. Geophys. Res. 97, 19749–19770.
Plank, T., Spiegelman, M., Langmuir, C.H., Forsyth, D.W., 1995. The meaning of 'mean F': clarifying the mean extent of melting at ocean ridges. J. Geophys. Res. 100, 15045–15052.
Pollack, H.N., 1986. Cratonization and thermal evolution of the mantle. Earth Planet. Sci. Lett. 80, 175–182.
Putirka, K.D., 1999. Melting depths and mantle heterogeneity beneath Hawaii and the East Pacific Rise: constraints from Na/Ti and rare earth element ratios. J. Geophys. Res. 104, 2817–2829.
Putirka, K.D., 2005. Mantle potential temperatures at Hawaii, Iceland, and the mid-ocean ridge system, as inferred from olivine phenocrysts: evidence for thermally driven mantle plumes. Geochem. Geophys. Geosyst. 6. doi:10.1029/2005GC000915.
Putirka, K.D., Perfit, M., Ryerson, F.J., Jackson, M.G., 2007. Ambient and excess mantle temperatures, olivine thermometry, and active vs. passive upwelling. Chem. Geol. 241, 177–206.
Roeder, P.L., Emslie, R.F., 1970. Olivine-liquid equilibrium. Contrib. Mineral. Petrol. 29, 275–289.
Shearer, C.K., Hess, P.C., Wieczorek, M.A., Pritchard, M.E., Parmentier, E.M., Borg, L.E., Longhi, J., Elkins-Tanton, L.T., Neal, C.R., Antonenko, I., Canup, R.M., Halliday, A.N., Grove, T.L., Hager, B.H., Lee, D.-C., Wiechert, U., 2006. Thermal and magmatic evolution of the Moon. Rev. Mineral. Geochem. 60, 365–518.
Shen, Y., Forsyth, D.W., 1995. Geochemical constraints on initial and final depths of melting beneath mid-ocean ridges. J. Geophys. Res. 100, 2211–2237.
Shih, C.-Y., Nyquist, L.E., Wiesmann, H., Reese, Y., Misawa, K., 2005. Rb-Sr and Sm-Nd dating of olivine-phyric shergottite Yamato-980459: petrogenesis of depleted shergottites. Antarc. Meteor. Res. 18, 46–65.
Smith, D., 2000. Insights into the evolution of the uppermost continental mantle from xenolith localities on and near the Colorado Plateau and regional comparisons. J. Geophys. Res. 2000, 16769–16781.
Sobolev, A.V., Hofmann, A.W., Sobolev, S.V., Nikogosian, I.K., 2005. An olivine-free mantle source of Hawaiian shield basalts. Nature 434, 590–597.
Solomatov, V.S., Moresi, L.N., 1996. Stagnant lid convection on Venus. J. Geophys. Res. 101, 4737–4753.
Stolper, E., Newman, S., 1994. The role of water in the petrogenesis of Mariana trough magmas. Earth Planet. Sci. Lett. 293–325, 293–325.
Stolper, E., Walker, D., Hager, B.H., Hays, J.F., 1981. Melt segregation from partially molten source regions: the importance of melt density and source region size. J. Geophys. Res. 86, 6261–6271.
Sugawara, T., 2000. Empirical relatioships between temperature, pressure, and MgO content in olivine and pyroxene saturated liquid. J. Geophys. Res. 105, 8457–8472.
Tamura, Y., Yuhara, M., Ishii, T., 2000. Primary arc basalts from Daisen Volcano, Japan: equilibrium crystal fractionation versus disequilibrium fractionation during supercooling. J. Petrol. 41, 431–448.
Taylor, R.N., Lapierre, H., Vidal, P., Nesbitt, R.W., Croudace, I.W., 1992. Igneous geochemistry and petrogenesis of the Izu-Bonin forearc basin. Proc. Ocean Drill. Program, Sci. Results 126, 405–430.
Ulmer, P., 2001. Partial melting in the mantle wedge — the role of H2O in the genesis of mantle -derived 'arc-related' magmas. Phys. Earth Planet. Inter. 127, 215–232.
van Keken, P.E., Kiefer, B., Peacock, S., 2002. High resolution models of subduction zones: implications for mineral dehydration reactions and the transport of water into the deep mantle. Geochem. Geophys. Geosyst. 3. doi:10.1029/2001GC000256.
Wang, K., Plank, T., Walker, J.D., Smith, E.I., 2002. A mantle melting profile across the Basin and Range, SW USA. J. Geophys. Res. 107 (1), 21.
Warner, R.D., Keil, K., Prinz, M., Laul, J.C., Murali, A.V., Schmitt, R.A., 1975. Mineralogy, petrology, and chemistry of mare basalts from Apollo 17 rake samples. Proc. Lunar Sci. Conf. 6, 193–220.
Wernicke, B., Spencer, J., 1999. Basin and Range extension. Spec. Pap. - Geol. Soc. Am. 338, 341–356.
West, M., Ni, J., Baldridge, W.S., Wilson, D., Aster, R., Gao, W., Grand, S., 2004. Crust and upper mantle shear wave structure of the southwest United States: implications for rifting and support for high elevation. J. Geophys. Res. 109. doi:10.1029/2003JB002575.
Workman, R.K., Hart, S.R., 2005. Major and trace element composition of the depleted MORB mantle (DMM). Earth Planet. Sci. Lett. 231, 53–72.
Yamaguchi, A., Clayton, R.N., Mayeda, T.K., Ebihara, M., Oura, Y., Miura, Y.N., Haramura, H., Misawa, K., Kojima, H., Nagao, K., 2008. A new source of basaltic meteorites inferred from Northwest Africa 011. Science 296, 334–336.
Yang, Y., Forsyth, D.W., 2006. Rayleigh wave phase velocities, small-scale convection, and azimuthal anisotropy beneath southern California. J. Geophys. Res. 111. doi:10.1029/2005JB004180.
Yin, Q.-Z., Jacobsen, S.B., Yamashita, K., Blichert-Toft, J., Telouk, P., Albarede, F., 2002. A short timescale for terrestrial planet formation from Hf-W chrnometry of meteorites. Nature 418, 949–952.
Zhong, S., Parmentier, E.M., Zuber, M.T., 2000. A dynamic origin for the global asymmetry of lunar mare basalts. Earth Planet. Sci. Lett. 177.